

# New results from an extensive aging test on bakelite Resistive Plate Chambers

G. Carboni<sup>a</sup>, G. Collazuol<sup>b</sup>, S. De Capua<sup>a</sup>, D. Domenici<sup>a</sup>, G. Ganis<sup>a</sup>, R. Messi<sup>a</sup>, G. Passaleva<sup>b\*</sup>, E. Santovetti<sup>a</sup>, M. Veltri<sup>c</sup>

<sup>a</sup>Università di Roma “Tor Vergata” and INFN – Roma II, Via della Ricerca Scientifica 1, I-00133 Roma, Italy

<sup>b</sup>Università di Firenze and INFN – Firenze, Via G. Sansone 1, I-50019, Sesto F.no, Firenze, Italy

<sup>c</sup>INFN–Firenze and Università di Urbino, V. S. Chiara 27, I-61029 Urbino, Italy

We present recent results of an extensive aging test, performed at the CERN Gamma Irradiation Facility on two single-gap RPC prototypes, developed for the LHCb Muon System. With a method based on a model describing the behaviour of an RPC under high particle flux conditions, we have periodically measured the electrode resistance  $R$  of the two RPC prototypes over three years: we observe a large spontaneous increase of  $R$  with time, from the initial value of about 2 M $\Omega$  to more than 250 M $\Omega$ . A corresponding degradation of the RPC rate capabilities, from more than 3 kHz/cm<sup>2</sup> to less than 0.15 kHz/cm<sup>2</sup> is also found.

## 1. INTRODUCTION

Resistive Plate Chamber (RPC) detectors have been proposed to cover a large fraction (about 48%) of the Muon System [1,2] of the LHCb experiment [3]. The LHCb apparatus covers the forward part of the solid angle and is therefore subject to a very large particle flux. In particular, the particle rates expected in the Muon System are significantly larger than those expected in the corresponding sub-detectors in ATLAS [4] and CMS experiments [5]. In the regions covered by RPCs, the maximum particle rate is expected to vary between 0.25 and 0.75 kHz/cm<sup>2</sup>, depending mainly on the polar angle. To cope with such high rates, LHCb RPCs are operated in avalanche mode [6,7,8], allowing to obtain a rate capability up to some kHz/cm<sup>2</sup> [9,10,11,12]. In these conditions, the rate capability of an RPC is determined by the volume resistivity  $\rho$  of the electrodes and scales roughly as  $1/\rho$ . For this reason, RPCs used in experiments working at high rates are generally built with bakelite electrodes, that can be produced with resistivities as low as 10<sup>9</sup>  $\Omega$ cm.

Variations of the electrode resistivity affect directly the rate capability of the RPCs: it is therefore very important to be able to monitor this parameter during the chamber operation. These variations can be due to changes in environmental parameters like temperature and humidity [13,14] or to possible aging effects due to operating conditions.

To study these effects, we have devised, in the framework of the aging studies for the LHCb muon chambers, an extensive series of tests which started in January 2001 and is expected to last until December 2002, exploiting the large CERN Gamma Irradiation Facility [15].

In this paper we present the latest results from these studies. Results from a systematic series of measurements of the resistivity of the bakelite electrodes of two RPC prototypes are presented. A study of the RPC rate capabilities is also discussed.

## 2. SETUP OF THE AGING TEST

The aging tests have been performed at the Gamma Irradiation Facility (GIF) at CERN. The

---

\*corresponding author

GIF is a test area where particle detectors are exposed to an adjustable photon flux from an intense  $^{137}\text{Cs}$  radioactive source with an activity of about 655 GBq. A muon beam from the SPS accelerator traverses the test area, so that various measurements can be performed on detectors in presence of the high background flux of photons from the source. In our case the source was also used to perform an accelerated aging test of the detectors [16]. A system of remotely controlled filters allows us to vary the photon rate by four orders of magnitude. The photon rate has been found to depend from the filter absorption factor  $Abs$  as  $\Phi = 1/Abs^{0.7}$

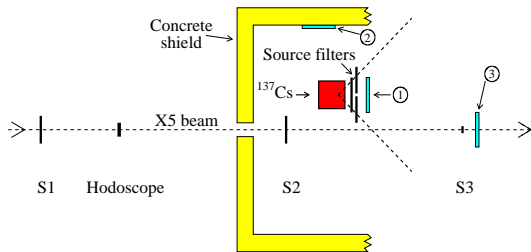


Figure 1. Schematic view of the test setup (not to scale). The positions of the RPCs corresponding to the various measurements are indicated (1-3). The distance of the RPC from the source in position 1 was about 55 cm, and in position 3 about 140 cm. The scintillator counters (S1-S3 and the Hodoscope) were used for measuring the RPC efficiency with the particle beam.

In our tests, two equal RPC detectors were operated in the GIF area. The detectors ( $50 \times 50 \text{ cm}^2$  with a 2 mm gas gap) were built using bakelite plates (2 mm thick) of nominal resistivity

$\approx 10^{10} \Omega\text{cm}$ , and treated internally with linseed oil.

Both detectors were operated with the same gas mixture, normally 95%  $\text{C}_2\text{H}_2\text{F}_4$ , 4%  $i - \text{C}_4\text{H}_{10}$  and 1%  $\text{SF}_6$ . High-voltage  $V_0$ , gas mixture composition, currents and temperature were continuously monitored and recorded during all the test period.

The test setup is schematically shown in Figure 1. Normally during the aging test one detector (RPC A) was placed in position 1, very close to the source and almost continuously exposed to radiation, whereas the second (RPC B) was placed far from the source (position 2), to serve as a reference.

Position 3 was used to perform efficiency measurements with the particle beam. In this case the signals from the RPCs were read out on 3 cm wide strips using fast electronics. A telescope of scintillator counters, also shown in Figure 1, provided the trigger and a hodoscope measured the particle position ( $x - y$ ) with an accuracy better than 1 cm. At the minimum source attenuation the measured flux density in Position 3 was about  $1 \text{ kHz/cm}^2$  [17].

### 3. BEHAVIOUR OF RPCs UNDER HIGH FLUX CONDITIONS

We have observed that the current drawn by RPC detectors subject to a high particle flux, shows a characteristic behaviour:

- it depends linearly on the applied voltage, above a certain threshold;
- it saturates with increasing flux values;
- it depends exponentially from the temperature at a fixed applied voltage.

We have interpreted these effects with a model, described in details in [18]. In this model we assume that the onset of the avalanche in the detector arises only above a threshold voltage  $V_T$ . Due to space charge effects, the avalanche charge depends linearly on the effective voltage  $V_{\text{gap}}$  across the gas gap:  $q \propto V_{\text{gap}} - V_T$ . Due to the voltage drop across the RPC electrodes, we have:

$V_{\text{gap}} = V_0 - IR$ , where  $V_0$  is the nominal applied voltage,  $I$  is the current drawn by the RPC and  $R$  is the total volume resistance of the two electrodes. The current  $I$  depends linearly on  $q$  through the incident flux  $\Phi$ :  $I = \Phi q(V_{\text{gap}})$ . In the limit of infinite flux, in order to keep the current finite, we should have  $V_{\text{gap}} = V_T$  and in these conditions we get a saturation value for the current  $I_{\text{max}} = (V_0 - V_T)/R$ . At finite flux values, one obtains [18]:

$$I = \left( \frac{X}{1+X} \right) \frac{V_0 - V_T}{R} = \frac{V_0 - V_T}{R_{\text{eff}}} \quad , \quad (1)$$

where  $X \propto \Phi R$  and  $R_{\text{eff}} = R(1+X)/X$ . Equation 1 is the central equation of the model: it shows that the current depends indeed linearly on  $V_0$  and that it saturates at high flux values and incorporates the temperature dependence of the current through the electrode resistance  $R$ .

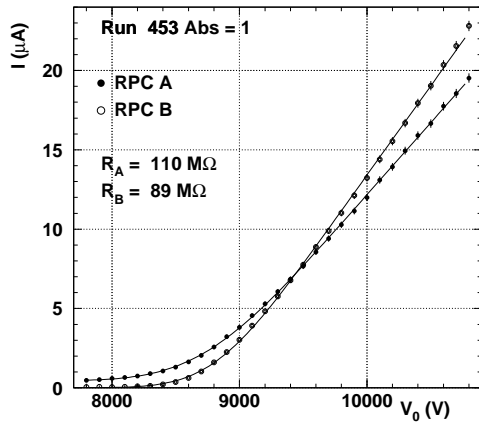


Figure 2. Current vs.  $V_0$  for RPC A (solid circles) and B (open circles) for absorption factor 1. The effective resistances  $R_{\text{eff}}$  as obtained from the slopes are also shown. In this case we had  $X = 49.8 \pm 8.9$ .

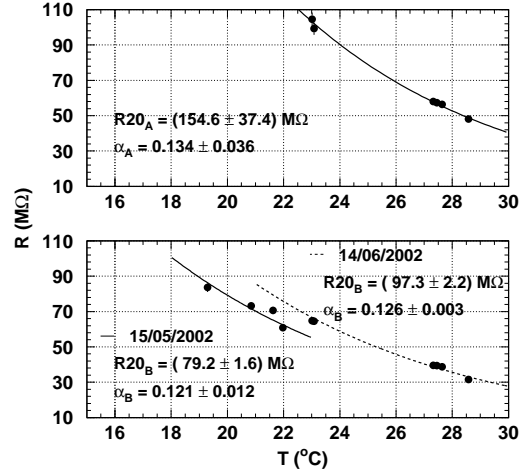


Figure 3. Resistances of RPC A and B plotted versus temperature. The temperature coefficient  $\alpha$  is fitted using an exponential dependence [18].

Typical  $I-V_0$  curves of the two detectors under test, taken for  $Abs = 1$  are shown in Figure 2. A perfect linearity is observed above the threshold voltage  $V_T$  (about 8500 V in this case). The resistance  $R$  can thus be measured by fitting these curves with Equation 1 and obtaining the parameter  $X$  by measuring the RPC current at fixed  $V_0$  for different flux values. In this way, the electrode resistance can be measured in a non destructive way and easily monitored during detector operation.

#### 4. RESULTS ON RPC RESISTANCE MEASUREMENTS

In the framework of the RPC aging tests, we have performed a systematic set of measurements of the RPC electrode resistances using the method described above.

In order to compare measurements taken at different ambient temperatures  $T$ , we have rescaled the values of  $R$  to 20°C assuming an exponen-

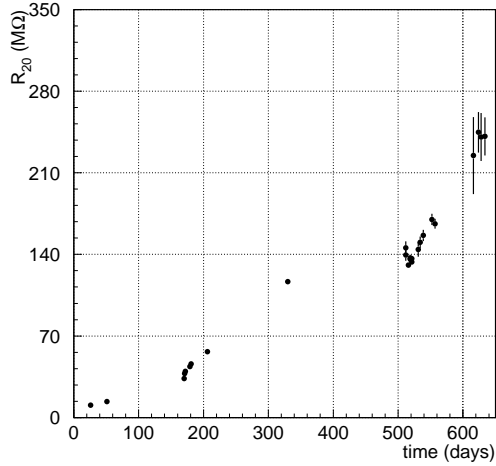


Figure 4. Measurements of  $R$  for RPC A versus time. The time scale starts at the beginning of the aging test in January 2001

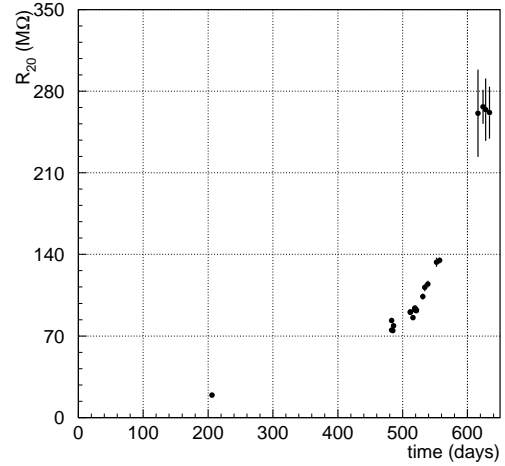


Figure 5. Measurements of  $R$  for RPC B versus time. The time scale starts at the beginning of the aging test in January 2001

tial dependence from  $T$  [18]. Figure 3 shows the measurement of  $R$  for the two RPCs at different temperatures. An exponential fit gives an average temperature coefficient of  $\langle \alpha \rangle = 0.126 \pm 0.008 \text{ } ^\circ\text{C}^{-1}$  in nice agreement with that obtained for the bakelite slabs themselves. This confirms that  $R$  is indeed the volume resistance of the RPC electrodes.

The measurements of  $R$  rescaled to  $20^\circ\text{C}$  are shown in Figure 4 and 5 for RPC A and RPC B respectively. The time scale starts at the beginning of the aging test in January 2001. In the first 200 days, RPC A was subject to an intense photon flux and integrated a charge of about  $0.4 \text{ C/cm}^2$  which corresponds to about 10 years of operation in LHCb [16]. As shown in Figure 6 the current drawn by the detector decreased by a factor of six in the same period. This behaviour was interpreted as a corresponding increase of the electrode resistance due to the current flowing through the electrodes themselves. This is indeed clearly visible in Figure 4. In the remain-

ing time, the chamber was again operated at the GIF but, because of the large resistance, the current drawn by the detector was negligible. Still, a large increase of  $R$  by another factor four is observed. This effect is confirmed by the measurements performed on the prototype B (Figure 5) that was exposed to the intense photon flux only for a short time. These results seem to indicate that the resistivity of the bakelite electrodes tends to spontaneously increase at a rate much larger than that observed when the RPCs are subject to the particle flux expected in the LHCb experiment. It is clear that this would be by far the main aging effect over 10 years of operation in LHCb.

We don't have yet a quantitative interpretation of these phenomena, although we believe that this is probably related to a decrease of water content in the bakelite plates. While water evaporation from the plates is always present, it is probably enhanced both by the current flowing in the electrodes and by the flux of dry gas in the chambers.

Table 1

Resistance  $R$  and rate capability  $r_{max}$  (see text) measured for RPC A in three different beam tests at the GIF. The values at 20 °C are obtained with a temperature coefficient  $\alpha = 0.126$  and scaling  $r_{max}$  like  $1/R$ .

Test	T (°C)	$R$ (M $\Omega$ )	$R(20^\circ\text{C})$ (M $\Omega$ )	$r_{max}$ (kHz/cm <sup>2</sup> )	$r_{max}(20^\circ\text{C})$ (kHz/cm <sup>2</sup> )
Oct. 1999	23.0	1.8	2.6	> 3	> 3
Aug. 2001	25.1	31.6	58.3	1.1	0.6
Jul. 2002	24.5	102.4	175.7	0.4	0.2

To cross-check this interpretation we are going to start a series of measurements, flushing our RPCs with a gas mixture containing water vapour.

## 5. ANALYSIS OF RATE CAPABILITIES

The maximum incident particle rate that an RPC can stand is roughly proportional to the inverse of the electrode volume resistivity. It is therefore essential to check what is the effect of the increase of the bakelite resistivity described

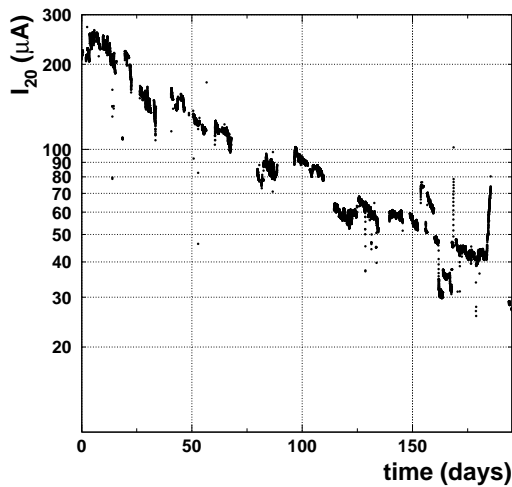


Figure 6. Current for RPC A corrected for temperature (see text) plotted versus time. The detector was placed at about 55 cm from the source.

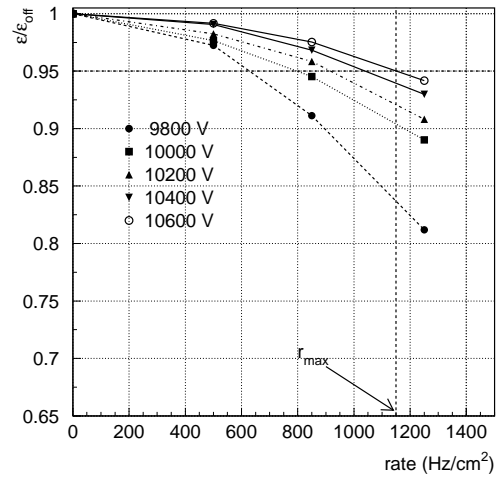


Figure 7. Efficiency vs. rate for RPC A, at different  $V_0$  values, measured in August 2001. The rate capability  $r_{max}$  is defined in the text.

above on the detector rate capability. To study quantitatively this effect, we define the rate capability  $r_{max}$  of our prototypes as the maximum rate where their efficiency is at least 95%, at a maximum operating voltage of 10.6 kV (this guarantees a plateau of about 400 V below the threshold of streamer regime), as shown in Figure 7. The results of three beam tests performed over a three years period are summarised in Table 1. In the 1999 test, the maximum available particle rate at the GIF was about 3 kHz/cm<sup>2</sup> but, at this

rate, the chamber efficiency was well above 95%; the rate capability was therefore much larger than 3 kHz/cm<sup>2</sup>. We can clearly see that the rate capability is dropping roughly as 1/ $R$  as expected. The rate capability extrapolated to the latest measurements of  $R$  is therefore about 0.15 kHz/cm<sup>2</sup> which is well below the rates foreseen in LHCb ( $> 0.25$  kHz/cm<sup>2</sup>). These results have recently brought the LHCb collaboration to abandon the RPC technology for the Muon System of the experiment.

## 6. CONCLUSIONS

We have developed and applied a method to measure RPC electrode resistance  $R$ , on-line, during chamber operations, in an easy and non destructive way. Using this method we have studied extensively the aging effects on bakelite RPCs. We have observed an increase of  $R$  by two orders of magnitude in about three years. Pure spontaneous aging is the dominant effect. The RPC rate capability dropped correspondingly from a few kHz/cm<sup>2</sup> to less than 0.15 kHz/cm<sup>2</sup>. These results brought the LHCb collaboration to abandon the RPC technology for the Muon System of the experiment.

## REFERENCES

1. The LHCb Collaboration, LHCb Muon System Technical design Report, CERN/LHCC 2001-010, 2001.
2. A. Bizzeti et al., Design and Construction of the RPC Detector for the LHCb Muon system, Note LHCb 2001-027, June 2001
3. The LHCb Collaboration, LHCb Technical Proposal, CERN/LHCC 98-4, 1998.
4. The ATLAS Collaboration, ATLAS Muon Spectrometer Technical Design Report, CERN/LHCC 97-22, 1997.
5. The CMS Collaboration, CMS Muon Technical Design Report, CERN/LHCC 97-32, 1997.
6. R. Cardarelli, A. Di Ciaccio and R. Santonico, Nucl. Instr. and Meth. A333 (1993) 399.
7. C. Bacci et al., Nucl. Instr. and Meth. A352 (1995) 552.
8. R. Cardarelli, V. Makeev, R. Santonico, Nucl. Instr. and Meth. A382 (1996) 470.
9. R. Cardarelli, Scientifica Acta VIII (Univ. Pavia), 3 (1993) 159.
10. M. Adinolfi et al., Nucl. Instr. and Meth. A456 (2000) 95.
11. R. Arnaldi et al., Nucl. Instr. and Meth. A456 (2000) 72.
12. M. Ćwiok et al., Nucl. Instr. and Meth. A456 (2000) 87.
13. R. Arnaldi et al., Nucl. Instr. and Meth. A456 (2000) 140.
14. I. Crotty et al., Nucl. Instr. and Meth. A346 (1994) 107.
15. S. Agosteo et al., Nucl. Instr. and Meth. A452 (2000) 94.
16. G. Passaleva et al., Proceedings of the “International Workshop on Aging Phenomena in Gaseous Detectors”, DESY, October 2001; [physics/0302029](#). Note LHCb 2003-013.
17. G. Ganis et al., Proceedings of the “VI Workshop on RPC and Related Detectors”, Coimbra, November 2001; [physics/0210045](#)
18. G. Carboni et al., “A model for RPC detectors operating at high rate”, to be published in Nucl. Instr. and Meth. A. Note LHCb-2002-069.